Investigation into the trade-off between part load fuel efficiency and transient response for a highly boosted downsized gasoline engine with CVT-supercharger

ATJM Rose[1], S Akehurst, CJ Brace

Abstract

Downsizing is an established trend in passenger car engine development. However, the benefits in improved fuel economy are often obtained at the expense of engine dynamic response (due to increasing demands on the boosting system), and, consequently, vehicle driveability. The use of a continuously variable transmission (CVT) in the supercharger driveline offers increased control flexibility over the air path which could allow more suitable calibrations to be developed.

This paper gives details of a co-simulation based investigation into the trade-off between steady state part load fuel efficiency and resulting tip-in transient response for a highly boosted downsized gasoline engine. The engine was a 2.0 litre in-line 4 cylinder unit, designed to replace a 5.0 litre naturally aspirated V8, equipped with a positive displacement supercharger in a sequential series arrangement with a fixed geometry turbocharger with external wastegate. The supercharger can be de-clutched and bypassed, and therefore three separate supercharger engagement regimes were investigated for part load operation – defined as: with the supercharger disengaged and bypassed; with the supercharger engaged with a fixed drive ratio; with the supercharger engaged using a variable ratio (i.e. through a CVT). For each of these supercharger engagement regimes, design of experiments and optimisation techniques were used to find the best settings for key engine control parameters such as intake and exhaust valve timing and EGR rate. Using these calibrations as a starting point, transient performance was then assessed in fixed speed tip-in simulations.

The trade-off situation was found to be highly complex; identifying the best overall balance of steady state efficiency and dynamic performance requires a subjective assessment. However, the CVT does provide the best potential for dynamic response combined with

---

[1] *Corresponding author:* Powertrain and Vehicle Research Centre, Department of Mechanical Engineering, University of Bath, Claverton Down, Bath BA2 7AY, UK. *Email:* A.T.J.Rose@bath.ac.uk

satisfactory fuel economy. It is suggested that the most suitable solution would be to have multiple user-selectable calibrations, such as ‘economy’ and ‘sport’ modes used on many modern vehicles.

Keywords

Internal combustion engine; spark ignition engine; downsizing; supercharging; turbocharging; continuously variable transmission; simulation.

1 Introduction

Under the pressure of constantly increasing global economic and legislative pressures faced by the automotive industry, engine downsizing and intake pressure charging has, according to Hancock et al. [1], ‘long been known as one of the most effective technologies for immediate implementation’. Engine downsizing is generally defined by Thirouard et al. [2] as using a ‘smaller capacity engine operating at higher specific engine loads in order to achieve lower fuel consumption’. The reduction in fuel consumption is achieved primarily through the inherently better efficiency of an engine when running at higher loads, and reduced friction losses associated with the reduced engine size [2]. Petitjean et al. [3] describe the former benefit as effectively ‘moving the best fuel economy island [of the engine] closer to the steady state road load condition’. Sliding surface friction is typically reduced through decreased piston ring to cylinder contact area (associated with a reduced number of cylinders and/or decreased bore and stroke) and a reduction in the swept area of crankshaft journal bearings. With increased levels of engine downsizing, however, one of the biggest technical challenges is maintaining good transient response [1], in keeping with consumer expectations of driveability.

This paper summarises an investigation into the trade-off between steady state part load efficiency – namely BSFC – and resulting tip-in transient response for a variety of control calibrations on a highly boosted downsized gasoline engine. The engine is a 2.0 litre in-line 4 cylinder unit, which has been conceived as a replacement for a 5.0 litre naturally aspirated V8 – the full load torque and power objectives are shown in Figure 1, along with the corresponding air mass flow requirements for the downsized engine. Further details of this project are available in [4]. The downsized engine features a pre-turbine to pre-compressor EGR circuit and both gasoline direct injection (GDI) and port fuel injection (PFI); its air charging system consists of a fixed geometry turbocharger (Honeywell GT30 with external wastegate) in a sequential series arrangement with a positive displacement supercharger (Eaton R410 Roots-type); the supercharger can be de-clutched and bypassed depending on

engine speed and load. A schematic of the engine is shown in Figure 2; engine geometry and other details are given in Table 1.

The overall aim of this particular downsizing project is a 35% reduction in fuel consumption (and corresponding reduction in CO_2) over the New European Drive Cycle (NEDC). For ease of analysis and comparison, the performance of the baseline V8 engine (as mounted in the target vehicle) over the NEDC has been discretized into a number of steady state 'Minimap' operating points – as described in [4]. Each of these points represents a portion of the drive cycle and holds a weighting equivalent to the proportion of time the engine is run at this speed and load during the NEDC. Using this method, drive cycle economy improvements can be estimated much more quickly.

Experimental data of a number of tip-in transient tests were also available for the baseline engine, which were used in the assessment of the performance of the downsized engine in the transient simulations.

2 Steady State Simulation

2.1 System Model

Engine performance was simulated using a 1D model implemented in the GT-Power engine simulation software package [5]; a schematic of the modelled engine is shown in Figure 2. Combustion was represented using a spark ignition Wiebe model; the Wiebe parameters used are typical of a naturally aspirated, 4-valve, port-injected, gasoline engine. Combustion effects such as knock and auto-ignition were ignored throughout since the operating points selected had been demonstrated experimentally to be achievable. The air-fuel ratio (AFR) control in the model was implemented by using direct injection only, the injectors being of an AFR-targeting type, set to achieve stoichiometry at all operating conditions – in accordance with the project target (defined in [4]). The primary load control mechanisms of the engine were thus as follows: the throttle valve; engagement of the supercharger, and its drive ratio; the turbocharger wastegate; the supercharger bypass valve; inlet and exhaust valve timing; and the EGR circuit valve. It is worth noting that spark timing would have been included in this list, but the Wiebe combustion model precludes this. Three separate supercharger engagement regimes were investigated for part load operation – these are defined as:

- with the supercharger disengaged and bypassed;
- with the supercharger engaged with a fixed drive ratio;
- with the supercharger engaged using a variable ratio (i.e. through a CVT).

2.2 Design of Experiments Parameter Optimisation

As a starting point for the investigation, Minimap point 3 (1500 rpm, 104 Nm [4], equating to 6.58 bar BMEP for the downsized engine) was chosen due to its high NEDC weighting value (as defined above) and reasonable load requirement – it is highly unlikely that the supercharger would be need to be engaged at loads lower than this. In order to find the optimal settings for the aforementioned load control mechanisms (valve timing, wastegate, etc.), a formal design of experiments (DoE) approach was adopted. The work was split into the three supercharger engagement regimes to allow a comparison of the optimal settings for each. The ranges of the seven input parameters are shown in Table 2.

The EGR rate in Table 2 was the target used in the EGR PID controller acting on a butterfly valve in the EGR circuit in the GT-Power model – defined as:

$$EGR\ Rate = \frac{MAF_{EGRvlv}}{MAF_{Throttle} + MAF_{EGRvlv}} \quad (1)$$

where $MAF_{Throttle}$ and MAF_{EGRvlv} are the mass airflows through the intake throttle and EGR valve, respectively. A high upper EGR target limit was used in order to test the boundaries of what is achievable with the system configuration used – in reality, lower values (<30%) would need to be used to retain combustion stability (which the simulations do not take into account) and to limit hydrocarbon emissions [6].

The wastegate and supercharger bypass diameters, for simplicity, were represented by variable orifice sections in the GT-Power model; in reality, flow control would likely be achieved by poppet and butterfly valves respectively. The supercharger bypass diameter was set to fully open when the supercharger was disengaged, and allowed to vary between its limits in the other instances. Valve timing limits were defined by the physical hardware used on the baseline engine. At this engine speed, standard intake valve maximum opening point (MOP) timing is 500 crank angle degrees (CAD) after top dead centre firing (ATDCF), with the ability to advance up to 63 degrees; standard exhaust valve MOP is 234 CAD ATDCF, with the ability to retard up to 50 degrees. Valve opening durations (fully closed to fully closed) around these MOPs are 202 and 216 degrees for inlet and exhaust respectively, giving a maximum possible overlap of 56 degrees. The fixed supercharger drive ratio was determined by the full load (WOT) requirements (Figure 1a); as for the range of CVT ratios, the upper value was set by the supercharger maximum speed (20000 rpm), and the lower value was selected to test the lower boundaries of operation and based on an extreme ratio range of 9:1. With all the other parameter values defined, a throttle PID controller was used within GT-Power to target the operating load of the selected Minimap point.

The Matlab Model Based Calibration (MBC) toolbox was used to develop the experimental test plan and to fit a response model to the resulting data. For the supercharger disengaged regime, an initial simulation screening experiment of 100 points of a grid-type 'optimal' design was used to fill the corners and outer edges of the design space; these were then augmented with 400 points determined using a Halton Sequence 'space-filling' design to maximise coverage of the variables' ranges in the most efficient way. For both the supercharger engaged and CVT regimes, the total number of experimental points was increased to 1000 to account for the additional variables used.

Considering the results from the GT-Power simulations, with extreme and unrealistic values filtered out, the responses of significant engine variables (such as BMEP and BSFC) were subsequently modelled. For the majority of the variables a neural network modelling approach was required due to the high complexity of the system – in part a result of the number of input parameters. Once the response models had been evaluated satisfactorily they were imported into the calibration generation (CAGE) element of MBC, to form the plant model for the subsequent optimisation process. The trade-off calibration feature within CAGE was used for this, which comprises filling in lookup tables for the various input parameters, with reference to the response models. Different tables (for example, intake against exhaust valve timing, supercharger drive ratio against bypass diameter) were completed and compared to see which parameters had the greatest effect on engine performance – particularly BSFC – and to collate the optimal settings that were found for each.

2.2.1 Optimised Steady State Parameter Settings

With the supercharger disengaged, the best BSFC was found to be approximately 240 g/kWhr, which was achieved with a high EGR target (30% and above), and the wastegate diameter set to 15 mm. As Figure 3 shows, the low BSFC region extends across a range of wastegate diameters (~3-19 mm) at high EGR targets; however, with the wastegate open less than 15 mm the BMEP target was unattainable. EGR targets above 30% were also disregarded for the same reason, or the EGR throttle was already fully open. Intake valve timing was advanced 50 degrees (to 450 CAD), and exhaust valve timing retarded by 21 degrees (to 255 CAD), giving an overlap of 14 degrees.

Similarly, with the supercharger engaged, the best BSFC was obtained with a high EGR target (again, 30% and above) and this was only slightly higher than with the supercharger disengaged at around 245 g/kWhr. As Figure 4 shows, the wastegate was fully closed at this operating point, with the BSFC benefit being derived from increased back pressure and, as a result, maximised EGR flow. As before, EGR targets above 40% were disregarded, as the EGR throttle was already fully open in this region. The supercharger bypass was partially

open (17 mm diameter out of a maximum 50 mm) to allow some flow recirculation and reduce the supercharger power consumption, but wider openings caused the BMEP to drop below the target value. Intake valve timing was fully advanced (to 437 CAD), and exhaust valve timing retarded by 21 degrees (to 255 CAD), giving an overlap of 27 degrees.

Considering the regime with the supercharger driven through a CVT, as would be expected, the drive ratio used had a major effect on overall efficiency, as shown in Figure 5. Consequently, a low drive ratio of 2:1 was chosen – lower than this gave no additional benefit. With this as a basis, a high EGR target again gave the best BSFC of approximately 251 g/kWhr, as shown in Figure 6, achieved with the wastegate fully open. By partially closing the wastegate, increased EGR flow could be achieved, resulting in equally good BSFC – as illustrated by the low BSFC region in Figure 6. However, adopting this strategy made the BMEP target difficult to attain and was therefore disregarded. For optimum operation, the supercharger bypass was partially open (16 mm diameter) again to allow some flow recirculation and reduce the supercharger power consumption. Intake valve timing was fully advanced (to 437 CAD), and exhaust valve timing retarded by 36 degrees (to 270 CAD), giving a considerable amount of overlap of 42 degrees.

Across the different supercharger engagement regimes, the parameter that had the largest independent effect on BSFC was the EGR target – increasing the EGR target was found to cause an almost linear reduction in BSFC, as can be seen in Figure 3, Figure 4 and Figure 6. As the level of EGR used was also expected to have a significant effect on the resulting dynamic response, two ‘optimum’ steady state calibrations for each supercharger engagement regime were taken forward to be used in the transient simulations – zero EGR and maximum EGR (i.e. fully open EGR throttle). A summary of the parameter settings for the resulting six calibrations is given in Table 3; for reference, predicted BSFC and percentage BSFC reduction (compared with the baseline engine) are also included. (It is worth noting that even the best BSFC reduction (20%) is some way off the overall target of 35%.)

3 Transient Simulation

The aim of this part of the investigation was to predict the response of the engine to a fixed speed tip-in transient – i.e. a step change in pedal demand from a low to a high value. This was to compare the transient performance commencing from each of the six part load calibrations detailed above with that of the baseline engine. Full load was used as the target for the tip-in – 438 Nm, equivalent to 27.7 bar BMEP for the downsized engine – with the step taking place over 0.15 seconds.

3.1 System Model

The GT-Power engine model used for the steady state simulations above was modified to perform a tip-in pedal event. The actual engine architecture was left largely unchanged from the arrangement described above. The EGR PID controller used for the various steady state EGR targets was removed and replaced with a time-dependent lookup table for the EGR throttle. For the three calibrations using EGR, this was set to fully open for the initial steady state period, then closed (with immediate response assumed) at the same rate as the 0.15 second step demand in BMEP; for the non-EGR calibrations, the EGR throttle was fully closed throughout. Time-dependent lookup tables were also put in place for the intake and exhaust timing values, the supercharger bypass diameter, and the turbocharger wastegate. For the latter two parameters the respective optimised steady state values were used initially, adjusting (at the same rate as above) to fully closed when full load was demanded (but then opening again – being used as the load control mechanism – when full load was achieved, as explained below). Similarly for the valve timings, the respective optimised steady state values were used initially, ramping linearly to the predetermined full load values at the start of the tip-in.

Regarding the supercharger, for the steady state regime with it engaged, the drive ratio was kept constant throughout the simulation, at the value of 5.9:1 determined by the full load torque curve requirements. For the supercharger disengaged regime, the drive ratio was set to zero initially, ramping up to 5.9:1 over the same 0.15 second period to represent the supercharger being clutched in. As with the other dynamic parameter adjustments, the actuator response was assumed to be instantaneous with respect to the step in pedal demand. Supercharger transmission efficiency was assumed to be 94%. For the steady state simulations of the configuration with variable supercharger drive, the drive ratio of the supercharger was simply manipulated to represent the CVT; for the transient simulations, however, a CVT element was incorporated into the GT-Power model to adequately represent the dynamic behaviour of the transmission. Mechanical efficiency of the CVT was assumed to be 95%, which combined with the aforementioned value for the supercharger drive (94%) gave an overall efficiency of 89%. Input and output shaft inertias were both assumed to be 5×10^{-4} kgm^2 (for comparison, the supercharger shaft inertia was 4.9×10^{-4} kgm^2), and a 20 ms time delay in the response of the CVT was used.

The GT-Power model was set up to run in a co-simulation environment with Matlab Simulink, to utilise the more sophisticated dynamic control structures available. Compared with using the throttle as the primary control mechanism, setting the throttle to fully open at the start of the tip-in (using a similar lookup table as for the other optimised parameters), and using a

common PID controller for the supercharger bypass valve and turbocharger wastegate was found to be a much more effective method of regulating the mass air flow (MAF) load (and thus the engine BMEP). For the CVT-driven supercharger, in conjunction with this control scheme, a similar manifold pressure-targeting PID controller for the CVT was found to be effective at providing acceptable transient behaviour. As with the parameter lookup tables, all controllers used were assumed to respond instantaneously to the step change in BMEP demand.

The simulation was set to run for seven seconds, with the tip-in occurring after four seconds to allow the model to achieve a steady state. A fixed value (corresponding to the respective optimised value – see Table 3) was used for supercharger bypass valve during the initial steady state period of the simulation, to ensure the correct setting was applied and to avoid unnecessary controller action and calibration. As both the supercharger bypass valve and turbocharger wastegate were controlled by the same signal, the signal was split within GT-Power and an appropriate gain applied to the branch leading to the wastegate, again to ensure the correct steady state setting. At the start of the tip-in the actuator signal was then switched within Simulink to the dynamic controller output, and the wastegate signal gain set to unity. The controller was of a proportional-integral (PI) type with anti-windup, and the PI values were manually calibrated for a satisfactory balance between speed of response and stability. The rate of actuator signal change was limited to an arbitrarily assumed value of +/- 350 mm/s, equivalent to going from fully open to fully closed in approximately 0.14 seconds. The same basic structure was used for the CVT-driven supercharger Simulink model, with a similar control loop used for the CVT as for the supercharger bypass valve and wastegate. Lower and upper limits for the CVT ratio were set at 2:1 and 13.3:1 (i.e. 20000 rpm supercharger speed limit divided by 1500 rpm engine speed) respectively. The rate of change was also limited to +/- 40 per second, equivalent to traversing the ratio range twice in one second.

3.2 Simulation Results and Discussion

3.2.1 Supercharger Disengaged and Engaged Regimes

Figure 7 shows a comparison of BMEP response between the supercharger engaged and disengaged regimes, both with and without EGR. As would be expected, BMEP response is delayed by both the use of EGR and by having the supercharger disengaged at the beginning of the transient; these two components of delay are essentially independent, although there are some interactions. Comparing T90 times (that is, time taken to achieve 90% of the step demand in BMEP), the delay resulting from having the supercharger initially disengaged is around 0.2 seconds. The time lag related to the use of EGR is most

pronounced in the first 0.6 seconds into the transient, at which point there is a marked dogleg in the BMEP responses; beyond this point the differences between the respective EGR and non-EGR settings are greatly reduced. Regarding the dogleg, there is also corresponding curvature in the non-EGR results, although much less pronounced. Without EGR, this dogleg phenomenon can be explained by the initial transient response being dominated by the supercharger performance (as shown in the pressure ratio traces in Figure 8), and after the maximum supercharger pressure ratio is reached the remaining performance is dominated by the turbocharger accelerating up to the required speed and pressure ratio (Figure 8b). With EGR, the dogleg is exaggerated by the time taken to clear the cylinders of residual exhaust gases happening concurrently with the supercharger acceleration. As Figure 9 shows, 0.6 seconds is needed to reduce in-cylinder EGR values to zero – with the presence of residual gases reducing the maximum achievable BMEP during the transient, in spite of comparable inlet manifold pressures as for the non-EGR settings (Figure 10). It is worth noting that, as Figure 9 shows, the simulations featured very high levels of EGR – up to 43%; in reality, lower values (<30%) would need to be used to retain combustion stability (which the simulations do not take into account) and to limit hydrocarbon emissions [6].

Figure 7 also shows experimental tip-in data for the baseline V8 engine – the recorded torque data has been adjusted to show the equivalent BMEP that would need to be produced by the downsized engine. Even though the baseline engine starts from a lower initial BMEP (around 4 bar compared with 6.58 bar), it achieves the 90% BMEP value more than 70% sooner than the downsized engine simulations, at around 0.3 seconds, with virtually linear behaviour up to the target. With the supercharger engaged at the start of the tip-in and running without EGR, performance is on a par with the baseline up until the aforementioned dogleg in BMEP at around 15 bar, demonstrating the beneficial instantaneous response provided by the supercharger. Although a direct comparison cannot be drawn between the experimental and simulated results, it does help to provide some context for the computed performance of the downsized engine.

The best simulated transient response also comes with a penalty in fuel efficiency. As Figure 11 shows, the best steady state (i.e. up to 4 seconds) BSFC results in the worst transient BMEP performance, and vice versa. (The steady state BSFC values reflect those obtained during the steady state optimisation procedure, shown in Table 3.) Further analysis of these results is discussed below.

3.2.2 CVT-Driven Supercharger

Adding the CVT-driven supercharger regime to the comparison reveals that – with or without EGR – it achieves the 90% BMEP value some 20% sooner than the other supercharger

engagement regimes, at approximately 0.9 seconds after the tip-in (Figure 7). Up until 0.75 seconds into the transient, however, the performance is in fact worse than the previously discussed supercharger regimes – below 0.5 seconds into the tip-in, it is significantly worse. In fact, the EGR operating condition shows a pronounced dip in BMEP at the start of the tip-in (to 4 bar, from the initial value of 6.58 bar), taking 0.5 seconds to recover and begin increasing beyond the initial steady state level; once recovered, a steeper rise in BMEP seems to be exhibited than the system without EGR. As with the other supercharger regimes, this initial difference between EGR and non-EGR settings is due to the time taken clearing the intake system and cylinders of the residual EGR gases (see Figure 9); once cleared, since the manifold pressure is already the same as the non-EGR system (Figure 10), and with the intake gases now 100% fresh air, the fuelling can quickly increase to catch up with the non-EGR system. The remainder of the initial performance deficit between the CVT and supercharger engaged regimes is down to the torque required to accelerate the supercharger – as with the supercharger disengaged regime, discussed above. However, the magnitude of this torque is much greater, as Figure 12 shows. The supercharger is accelerated from its steady state speed (3000 rpm) up to a maximum of around 14000 rpm, compared with the previous maximum of 8850 rpm, and this is combined with the added inertia of the CVT and its accompanying mechanical efficiency reduction.

At the end of the transient, the BSFC of the CVT-driven supercharger scheme is worse than that of the previous configurations, due to the supercharger producing a larger share of the overall boost pressure – see Figure 8 and Figure 11. As the target BMEP is achieved earlier, the turbocharger has less time to accelerate before the wastegate is opened, resulting in lower turbocharger speed and higher supercharger speed. Increased steady state parasitic losses are an outcome of the higher supercharger speed that is required, meaning that a higher manifold pressure is needed to produce the same BMEP – see Figure 10 and Figure 12. This issue could be rectified with a more sophisticated controller calibration for the full load steady state conditions, bringing the BSFC in line with the other supercharger regimes; for the purposes of this investigation the current set up is sufficient, however, as the initial steady state and dynamic performance is the focus.

Overall, it is fair to say that the optimised steady state settings for the CVT-driven supercharger regime resulted in fairly poor dynamic performance in the tip-in simulations. As this can largely be attributed to the low initial supercharger drive ratio used an alternative setup was considered, using a higher steady state drive ratio of 5.9:1 – in line with the other supercharger regimes. Dynamic performance was greatly improved using this arrangement, reaching the 90% BMEP value some 40% sooner than the original supercharger

engagement regimes, and 25% sooner than with an initial drive ratio of 2:1, at approximately 0.7 seconds after the tip-in (Figure 13). The almost-linear nature of the BMEP trace is also similar to that of the equivalent baseline experimental data discussed earlier – though with the response time doubled.

Nevertheless, the previously listed disadvantages of the CVT-driven supercharger configuration have not been totally eradicated. For instance, up until 0.5 seconds into the tip-in the BMEP produced remains inferior to that of the supercharger engaged regime (for the same reasons as mentioned above – the vastly increased torque required to accelerate and keep the supercharger at high speed, as shown in Figure 12). With EGR, a slight dip in BMEP below the initial steady state level is still exhibited for the first 0.4 seconds – although it is significantly better than the former CVT-supercharger setup (Figure 13). The final steady state BSFC also suffers from the same problem as before (Figure 11), resulting from the supercharger taking a larger proportion of the boosting work than necessary (Figure 8) – but again this could be solved with better controller calibration. Furthermore, the improved dynamic performance comes at the expense of worsened initial BSFC compared with using a steady state CVT ratio of 2:1 (with or without EGR), as shown in Figure 11.

Considering the transient operating points on the turbocharger compressor map (Figure 14a – non-EGR data only plotted, for clarity), all of the simulations inhabit the bottom left region of low pressure ratio and low mass flow. Since this is where the map data is most extrapolated, this adds another layer of uncertainty about the reliability of the modelling predictions. However, the corresponding operating points on the supercharger map are more central, giving more confidence (Figure 14b).

3.2.3 Rise Time Analysis

The complex nature of the simulation results necessitates a multifaceted approach for performance evaluation. As well as the relatively straightforward appraisal of the BMEP performance discussed above, rise time measurements and driveability assessment techniques were used. Firstly, considering the T10 values (that is, time taken to achieve 10% of the step demand in BMEP) of the various simulations against their respective initial steady state BSFC values, the supercharger engaged non-EGR regime clearly has the fastest initial response (Figure 15), but practically the worst BSFC; conversely, the supercharger engaged EGR regime has the best BSFC, but a significantly worse T10 time. A Pareto optimal front can be drawn using this data (the black dashed line in Figure 15), to show where the highest Pareto efficiency is achieved. In this case there is a roughly linear inversely proportional relationship between steady state BSFC and initial transient response, and the non-CVT supercharger regimes can be considered the most Pareto-efficient (i.e. closest to or on the

Pareto optimal front). On the other hand, the CVT-supercharger points could not be shifted closer to the Pareto optimal front without sacrificing either steady state BSFC or T10 time. Considering the EGR and non-EGR points of any given supercharger regime shows a clear trade-off between steady state BSFC and initial transient response – the same inversely proportional trend as displayed in the Pareto optimal front is visible in each case. The same can also be said of the initial supercharger speed (i.e. CVT ratio) of the equivalent CVT simulations, or having the supercharger engaged (for the non-CVT simulations) – improved transient response comes at the cost of worse efficiency. Each of these conclusions is consistent with those made in the previous sections but do not reveal the full picture of the respective performances; further complementary analysis is required.

An assessment of the corresponding T90 times (i.e. time to achieve 90% of the BMEP step demand) essentially shows a complete reversal (Figure 16), with the CVT-supercharger regimes the most Pareto-efficient – in terms of T90 time at least. The supercharger disengaged EGR point also features on the Pareto optimal front, but with a greatly increased T90 time and only slightly reduced BSFC (compared with the 2:1 CVT-supercharger with EGR condition). Again there is an interesting relationship between the EGR and non-EGR points of each supercharger engagement regime; using EGR gives a significant reduction in initial BSFC (8-13%), but approximately the same T90 time is achieved with or without EGR. As discussed previously, however, initial transient response deteriorates when using EGR. In terms of absolute Pareto-efficiency for T90 time versus BSFC, the two CVT-supercharger settings with EGR appear supreme.

Figure 17 shows the T10-T90 values (i.e. time taken to go from 10% to 90% of the BMEP step demand) for each of the simulations. A similar trend as to the T90 times (Figure 16) is displayed, but here the advantage of the CVT-supercharger regimes compared with those with fixed drive ratio is particularly clear – the T10-T90 times of the former are around 60% lower. A similar relationship between the EGR and non-EGR points of each supercharger engagement regime is also displayed (Figure 17); using EGR gives a significant reduction in initial BSFC (8-13%), accompanied by a comparable T10-T90 time (if anything, slightly lower). As mentioned previously, the EGR rates used in these simulations are higher than would be used in reality; however, the trends shown in these graphs can be interpreted as vectors (Figure 15, Figure 16, Figure 17), and thus reducing the level of EGR would simply shift the operating point along the vector towards the corresponding non-EGR result.

Taking the T90 and T10-T90 metrics in isolation, the CVT-supercharger regimes with EGR are clearly the most Pareto-efficient, providing the best balance between BSFC and dynamic performance; but again, this must interpreted in the context of the initial time to BMEP

fluctuation (T10 times, Figure 15), where the CVT-supercharger regimes faired significantly worse. The performance appraisal may benefit from additional driveability assessments.

3.2.4 Driveability Analysis

As Pickering and Brace [7] state, ‘driveability is by its nature a subjective rating’, and is hence difficult to quantify. Studies have been performed into the correlation between subjective assessments and objective measurements of vehicle behaviour [8][9][10][11]; with regards to tip-in performance and assessment of launch feel, List and Schoeggl [8] and Wicke et al. [10] have identified delay time, acceleration, and jerk (defined as a measure of initial rate of change of acceleration) as key metrics for these correlations. These studies were based on in-vehicle tests, as opposed to fixed speed tip-in simulations in the current investigation, and hence the conclusions pertaining to acceleration and jerk are inapplicable. Also, time delay was defined as the time between change in pedal demand and first change in vehicle acceleration [10]; however, it is expected that likening this to the delay in engine response to the BMEP demand in the simulations will give at least an indication of the driveability of the different boosting configurations when mounted in a vehicle. On this basis, the findings of Wicke et al. [10] that a delay time of less than around 350 ms is necessary to achieve a good subjective driveability rating can be applied as a criterion for the simulations in this investigation. Thus, considering the percentage increase in BMEP at this key period during the tip-in (Figure 18), with the possible exception of the supercharger engaged and disengaged regimes, the configurations with EGR provide inadequate performance; the supercharger engaged regime without EGR is clearly the best from a driveability point of view, with some competition from the supercharger disengaged and CVT-supercharger (with 5.9:1 steady state ratio) regimes. Plotting these results against the respective steady state BSFC values gives another perspective (Figure 19) – highlighting the relative inefficiency of the SC engaged and CVT-supercharger regimes, and bringing to the fore the balance between driveability and efficiency provided by the supercharger disengaged regime. These conclusions must of course be made tentatively; the applicability of the delay time driveability criterion to fixed speed simulations and the assumed immediate response of controllers and parameter changes in the model necessitate caution. However, the relative merits of the different configurations are fairly clear.

4 Conclusions

The trade-off between steady state part load fuel efficiency and resulting tip-in performance has been investigated for a highly boosted downsized gasoline engine. Since the engine uses a fixed geometry turbocharger (with external wastegate) in a sequential series arrangement with a positive displacement supercharger, three different supercharger

engagement regimes were considered: with the supercharger disengaged and bypassed; with the supercharger engaged with a fixed drive ratio; with the supercharger engaged using a variable ratio (i.e. through a CVT). Focussing on an operating point of 1500 rpm and 104 Nm (equivalent to 6.58 bar BMEP), design of experiments and optimisation techniques were used to find the best settings for the various engine control parameters. Of these parameters, target EGR rate was found to have the largest independent effect on BSFC – increasing the EGR target was found to cause an almost linear reduction in BSFC. However, it was expected that the level of residual gases present would have a large effect on tip-in performance; hence for each supercharger engagement regime, two modes of operation (zero EGR and maximum achievable EGR) were taken forward for evaluation in the transient simulations.

Dynamic performance was simulated in a GT-Power/Matlab Simulink co-simulation environment in order to utilise the more sophisticated dynamic control structures available within Simulink. Using each of the six part load calibrations, a fixed speed tip-in transient was performed, demanding full load (438 Nm, 27.7 bar BMEP) with the step taking place over 0.15 seconds. Evaluating the dynamic performance of the different operating regimes was a complex process; even ignoring steady state BSFC, none of the calibrations was entirely superior to the others. Compared with experimental data for the baseline engine, none of the downsized configurations were able to achieve equivalent performance. Initial response was best with the supercharger engaged, but the total time to reach the BMEP target was poor; conversely, the CVT-supercharger set up (with the same steady state drive ratio) achieved the BMEP target much sooner, but sacrificed initial BMEP response in the process. As anticipated, settings with EGR showed worse performance – particularly in the initial response period – but compensated with reduced (by 8-13%) steady state BSFC. Driveability metrics were also considered, which indicated that the supercharger engaged arrangement (without EGR) would likely result in the greatest subjective rating – at the cost of the worst BSFC.

In summary, the trade-off situation was found to be more complex than first anticipated; identifying the best overall balance of steady state efficiency and dynamic performance requires a subjective assessment. However, the CVT does provide the best potential for dynamic response combined with satisfactory fuel economy – there would be scope to improve fuel economy further by initially disengaging the CVT-supercharger, at the expense of marginally reduced transient performance. Perhaps the most suitable solution would be to have multiple user-selectable calibrations, such as ‘economy’ and ‘sport’ modes used on many modern vehicles.

Acknowledgements

The authors would like to thank the Engineering and Physical Sciences Research Council (EPSRC) for funding this research, and the UK Technology Strategy Board (TSB) for their funding and support for the Ultraboost project. The authors would also like to acknowledge the Ultraboost consortium partners: Jaguar Land Rover, Lotus Engineering, GE Precision Engineering, Imperial College London, the University of Leeds, CD-adapco, and Shell Fuels.

References

[1] **Hancock, R., Fraser, N., Jeremy, M., Sykes, R.** and **Blaxill, H.** A New 3 Cylinder 1.2l Advanced Downsizing Technology Demonstrator Engine. SAE paper 2008-01-0611, 2008.

[2] **Thirouard, M., Mendez, S., Pacaud, P., Chmielarczyk, V., Ambrazas, D, Garsi, C., Lavoisier, F.** and **Barbeau, B.** Potential to Improve Specific Power Using Very High Injection Pressure in HSDI Diesel Engines. SAE paper 2009-01-1524, 2009.

[3] **Petitjean, D., Bernardini, L., Middlemass, C.** and **Shahed, S.M.** Advanced Gasoline Engine Turbocharging Technology for Fuel Economy Improvements. SAE paper 2004-01-0988, 2004.

[4] **Carey, C., McAllister, M., Sandford, M., Richardson, S., Pierson, S., Darnton, N., Bredda, S., Akehurst, S., Brace, C., Turner, J., Pearson, R., Luard, N., Martinez-Botas, R., Copeland, C., Lewis, M.** and **Fernandes, J.** Extreme engine downsizing. In International Conference on *Innovations in Fuel Economy and Sustainable Road Transport*, Pune, India, 8-9 November 2011 (Professional Engineering Publishing, London).

[5] **Gamma Technologies Inc.** *GT-POWER Engine Simulation Software* [online], 2012. Available from: http://www.gtisoft.com/applications/a_Engine_Performance.php [Accessed 13 December 2012].

[6] **Heywood, J.B.** *Internal Combustion Engine Fundamentals*, 1988 (McGraw-Hill, New York).

[7] **Pickering, S.G.** and **Brace, C.J.** Automated data processing and metric generation for driveability analysis. *Proceedings of the Institution of Mechanical Engineers, Part D: Journal of Automobile Engineering*, 2007, **221**(4), 429-441.

[8] **List, H.O.** and **Schoeggl, P.** Objective Evaluation of Vehicle Driveability. SAE paper 980204, 1998.

[9] **Dorey, R.E.** and **Holmes, C.B.** Vehicle Driveability - Its Characterisation and Measurement. SAE paper 1999-01-0949, 1999.

[10] **Wicke, V., Brace, C.J.** and **Vaughan, N.D.** The Potential for Simulation of Driveability of CVT Vehicles. SAE paper 2000-01-0830, 2000.

[11] **Dorey, R.E.** and **Martin, E.J.** Vehicle Driveability - The Development of an Objective Methodology. SAE paper 2000-01-1326, 2000.

Appendix

Acronyms

AFR	air-fuel ratio
ATDCF	after top dead centre firing
BMEP	brake mean effective pressure
BSFC	brake specific fuel consumption
CAD	crank angle degrees
CAGE	Calibration Generation
CO_2	carbon dioxide
CVT	continuously variable transmission
DoE	design of experiments
EGR	exhaust gas recirculation
GDI	gasoline direct injection
MAF	mass air flow
MBC	Model-Based Calibration Toolbox
MOP	maximum opening point
NEDC	New European Drive Cycle
PFI	port fuel injection
PI	proportional-integral (control)
PID	proportional-integral-derivative (control)
SC	supercharger
TC	turbocharger
WOT	wide open throttle

Notation

$\dot{m}$	mass air flow (kg/s)
P	pressure (N/m^2)
T	temperature (K)

Tables

Table 1 – Downsized engine parameters

Parameter	*Value*
Bore (mm)	83
Stroke (mm)	92
Displacement (cc)	1991
Con Rod Length (mm)	150
Compression Ratio	9:1
Max Power (kW) @ Rated Speed (rpm)	283, 6500
Max Torque (Nm) @ Rated Speed (rpm)	515, 3500

Table 2 – Design of Experiments factors

Parameter	*SC disengaged*	*SC engaged*	*SC CVT*
Wastegate diameter (mm)	0 – 21	0 – 21	0 – 21
Target EGR rate (%)	0 – 50	0 – 50	0 – 50
Intake valve MOP (CAD ATDCF)	437 – 500	437 – 500	437 – 500
Exhaust valve MOP (CAD ATDCF)	234 – 284	234 – 284	234 – 284
SC bypass diameter (mm)	50	0 – 50	0 – 50
SC drive ratio	0	5.9	1.5 – 13
Throttle angle (deg)	PID controlled (BMEP target)		

Table 3 – Optimised steady state parameter settings

Parameter	*SC disengaged*		*SC engaged*		*SC CVT*	
	EGR	*No EGR*	*EGR*	*No EGR*	*EGR*	*No EGR*
EGR throttle angle (deg)	90	0	90	0	90	0
Wastegate diameter (mm)	15	15	0	0	21	21
Intake valve MOP (CAD ATDCF)	450	437	437	443	437	470
Exhaust valve MOP (CAD ATDCF)	255	245	255	234	270	234
Valve overlap (deg)	14	17	27	0	42	0
SC bypass diameter (mm)	50	50	17	21	16	19
SC drive ratio	0	0	5.9	5.9	2	2
BSFC (g/kWhr)	*240*	*264*	*245*	*282*	*251*	*261*
Predicted BSFC reduction (%)	*20*	*12*	*18*	*6*	*16*	*13*

Figures

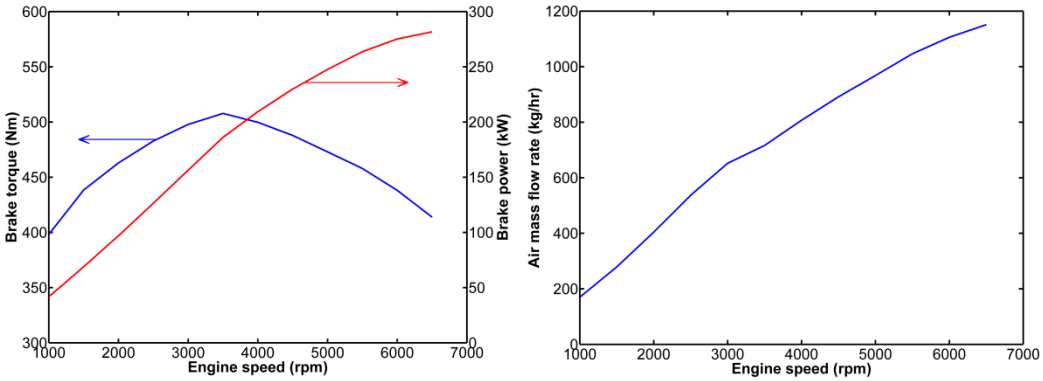

Figure 1 – Downsized engine performance requirements – a) torque and power; b) air mass flow

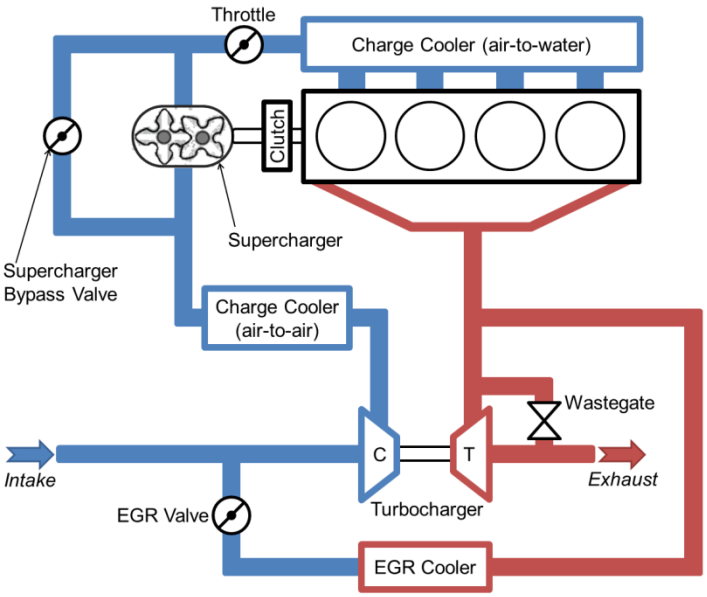

Figure 2 – Downsized engine schematic

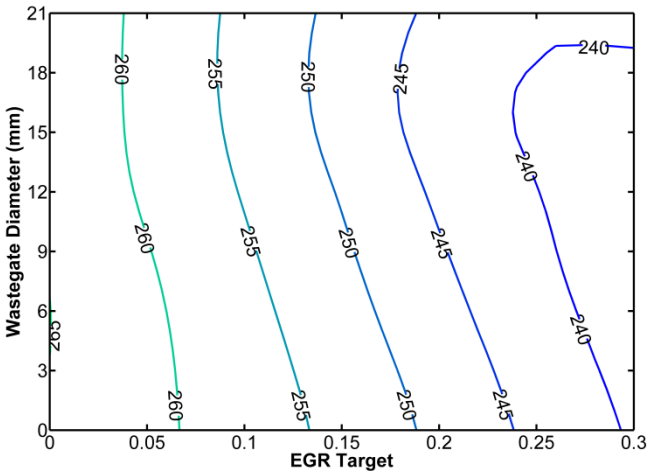

Figure 3 – Supercharger disengaged regime steady state parameter optimisation – contours of BSFC (in g/kWhr) for the trade-off between wastegate diameter and EGR target

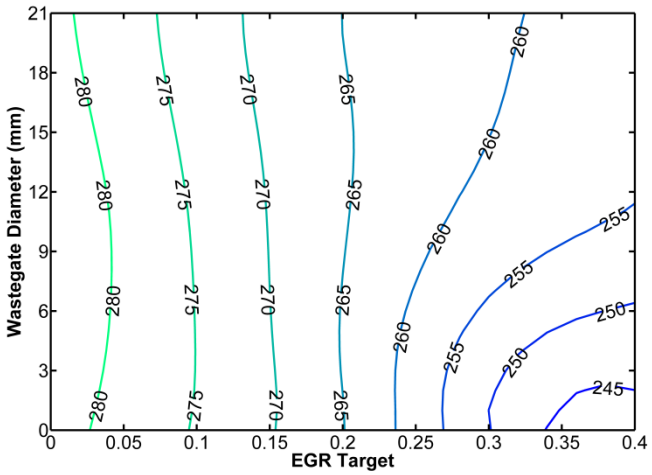

Figure 4 – Supercharger engaged regime steady state parameter optimisation – contours of BSFC (in g/kWhr) for the trade-off between wastegate diameter and EGR target

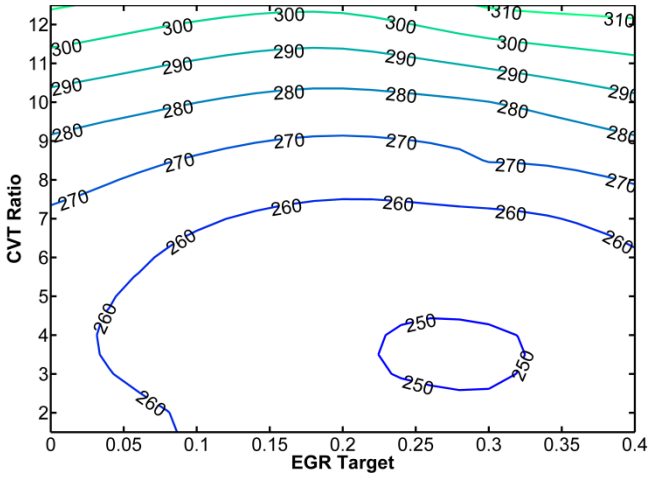

Figure 5 – CVT-driven supercharger regime steady state parameter optimisation – contours of BSFC (in g/kWhr) for the trade-off between CVT ratio and EGR target

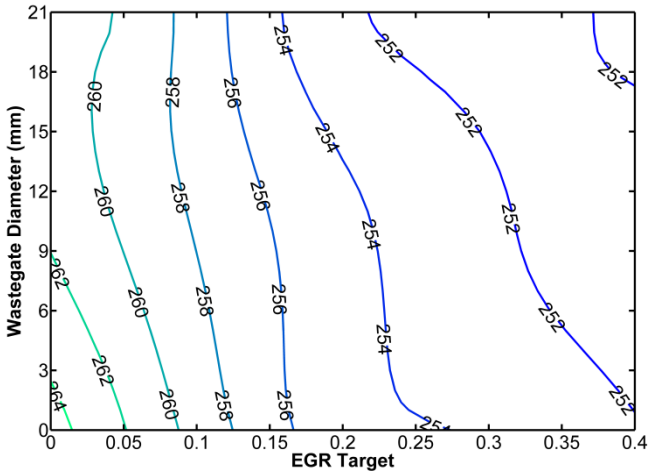

Figure 6 – CVT-driven supercharger regime steady state parameter optimisation – contours of BSFC (in g/kWhr) for the trade-off between wastegate diameter and EGR target (N.B. CVT ratio fixed at 2:1)

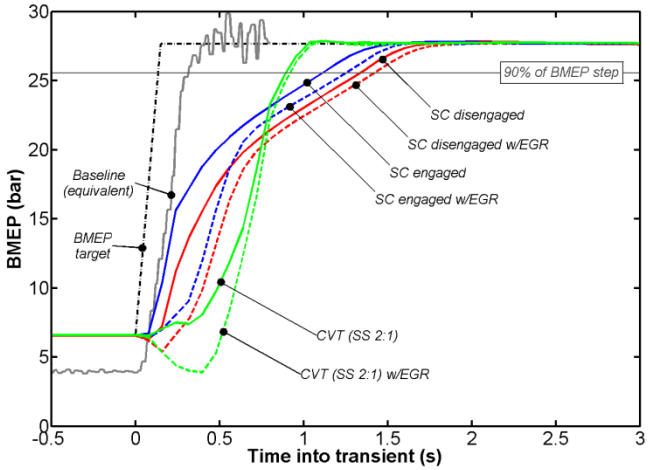

Figure 7 – Brake mean effective pressure (BMEP) response for tip-in simulations of supercharger (SC) engaged, supercharger disengaged, and CVT-driven supercharger regimes. For reference BMEP target, 90% of BMEP step demand, and equivalent BMEP for baseline experimental results are also shown

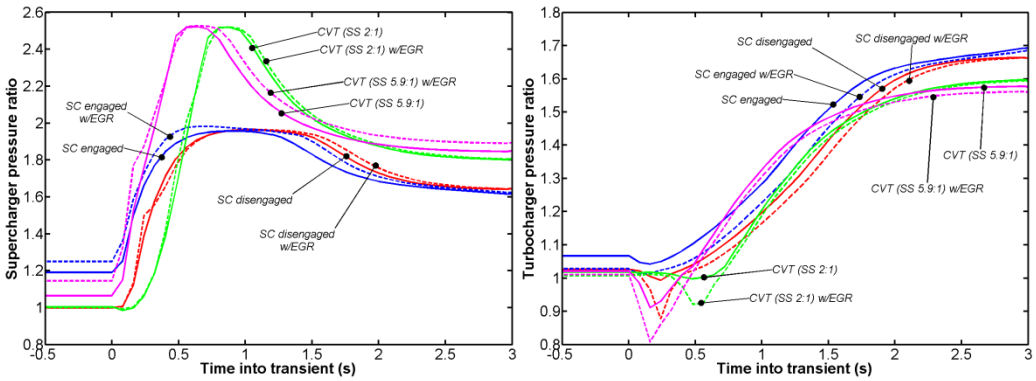

Figure 8 – Individual compressor pressure ratios for tip-in simulations of supercharger engaged, supercharger disengaged, and CVT-driven supercharger regimes – a) supercharger; b) turbocharger

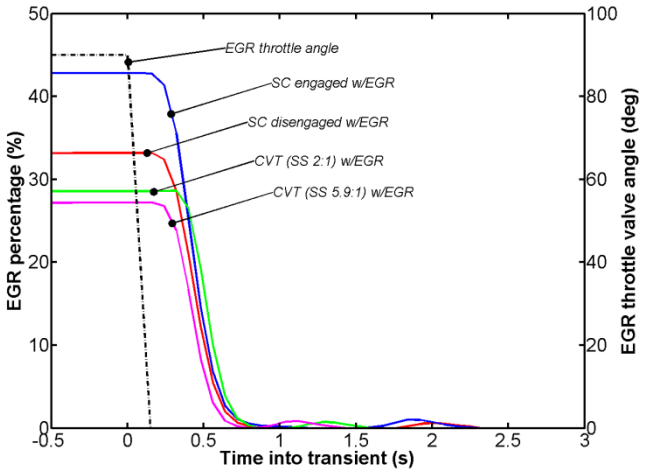

Figure 9 – In-cylinder EGR percentages for tip-in simulations of supercharger engaged, supercharger disengaged, and CVT-driven supercharger regimes (with EGR). For reference, EGR valve angle is also shown

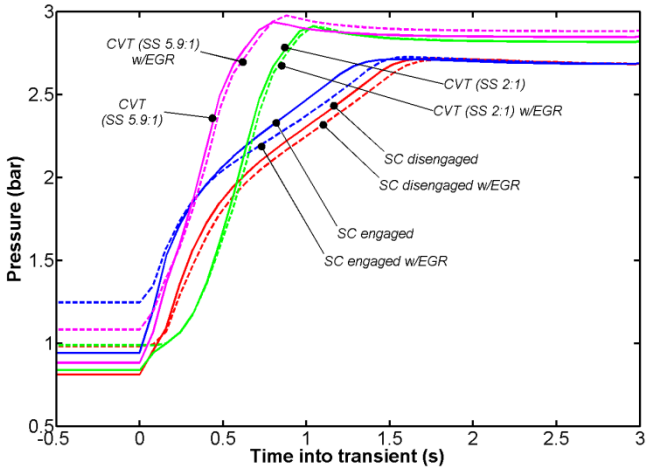

Figure 10 – Inlet manifold pressures for tip-in simulations of supercharger engaged, supercharger disengaged, and CVT-driven supercharger regimes

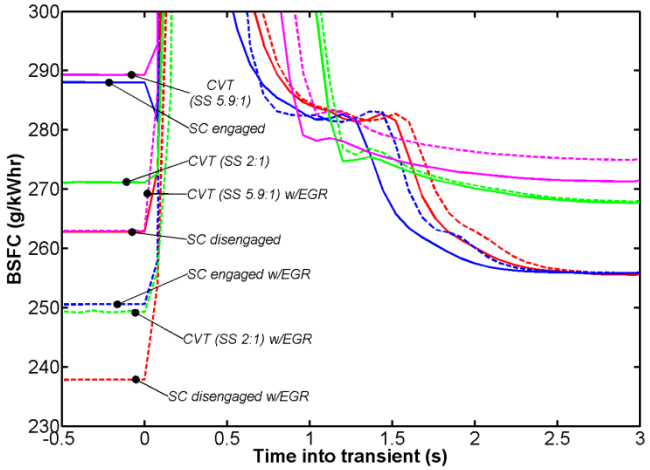

Figure 11 – Brake specific fuel consumption (BSFC) for tip-in simulations of supercharger engaged, supercharger disengaged, and CVT-driven supercharger regimes

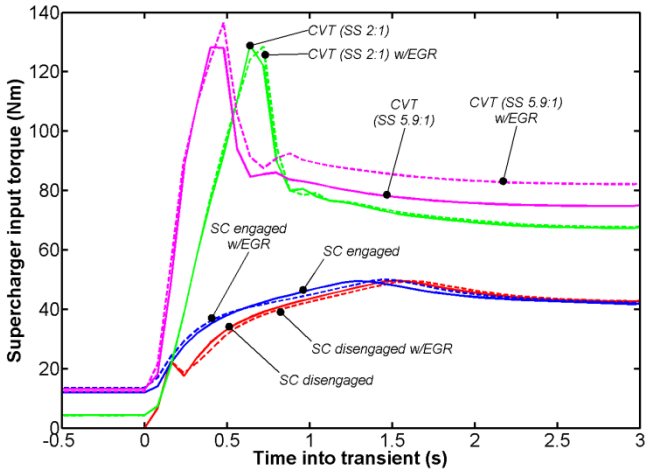

Figure 12 – Supercharger input torques for tip-in simulations of supercharger engaged, supercharger disengaged, and CVT-driven supercharger regimes

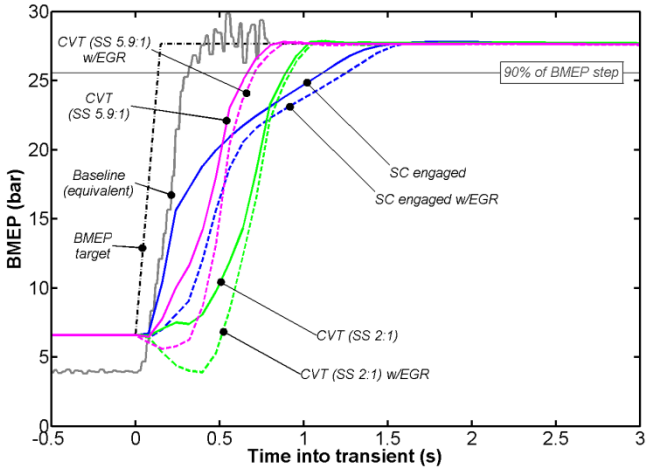

Figure 13 – Brake mean effective pressure (BMEP) response for tip-in simulations of supercharger (SC) engaged and CVT-driven supercharger regimes, showing the effect of initial steady state CVT ratio. For reference BMEP target, 90% of BMEP step demand, and equivalent BMEP for baseline experimental results are also shown

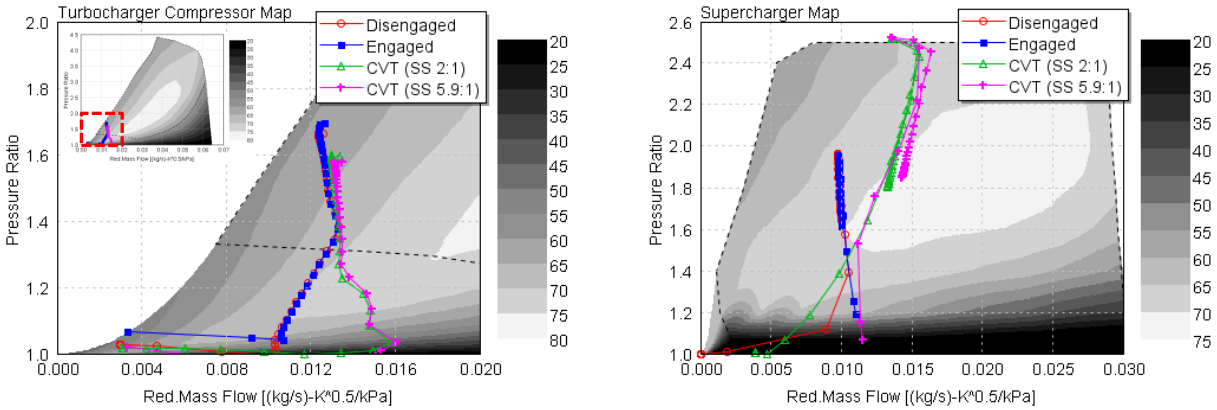

Figure 14 – Compressor maps with transient operating points (showing non-EGR data only, for clarity) – a) turbocharger; b) supercharger. Shaded contours show compressor isentropic efficiency (%). Horizontal axis is the reduced mass flow parameter $\frac{\dot{m}\sqrt{T_{inlet}}}{P_{inlet}}$, which is independent of inlet conditions (i.e. temperature and pressure)

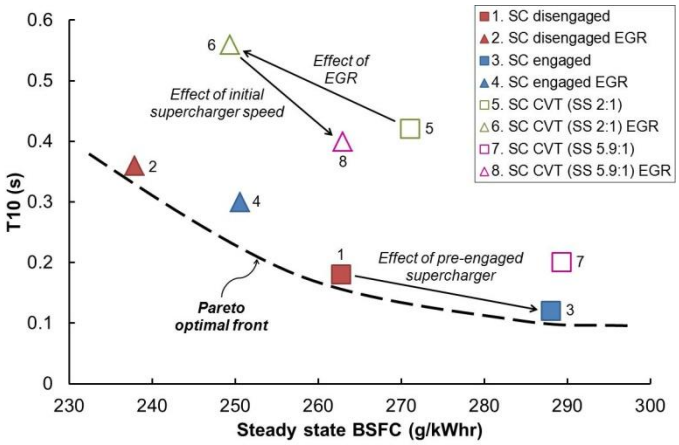

Figure 15 – Rise time analysis – T10 (time to achieve 10% of the step demand in BMEP) against initial steady state BSFC

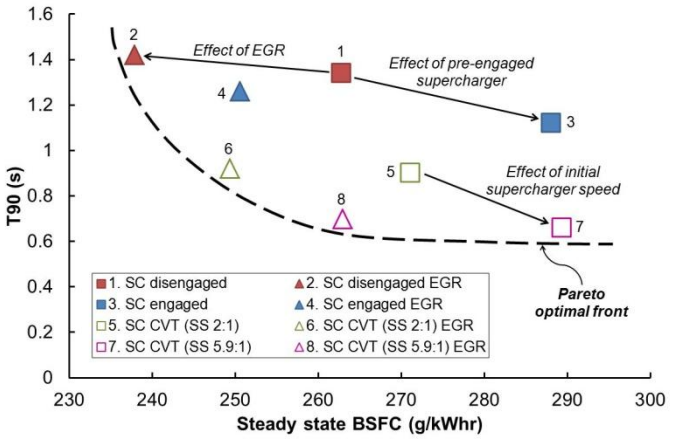

Figure 16 – Rise time analysis – T90 (time to achieve 90% of the step demand in BMEP) against initial steady state BSFC

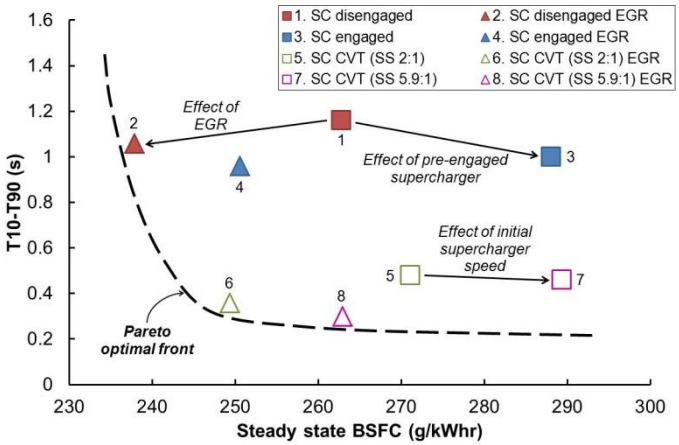

Figure 17 – Rise time analysis – T10-T90 (time taken to go from 10% to 90% of the BMEP step demand) against initial steady state BSFC

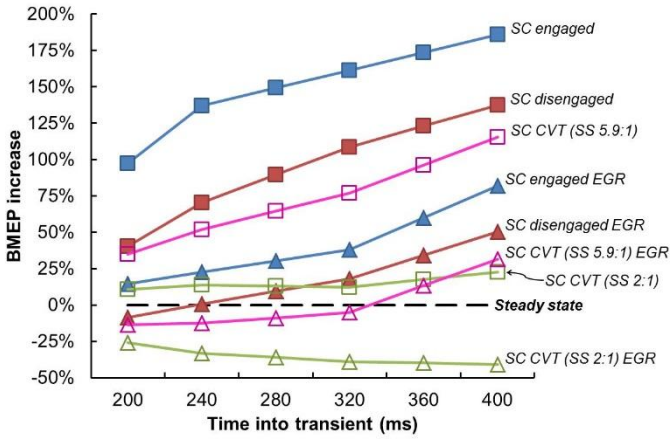

Figure 18 – Driveability analysis – percentage BMEP increase at key times during tip-in transient

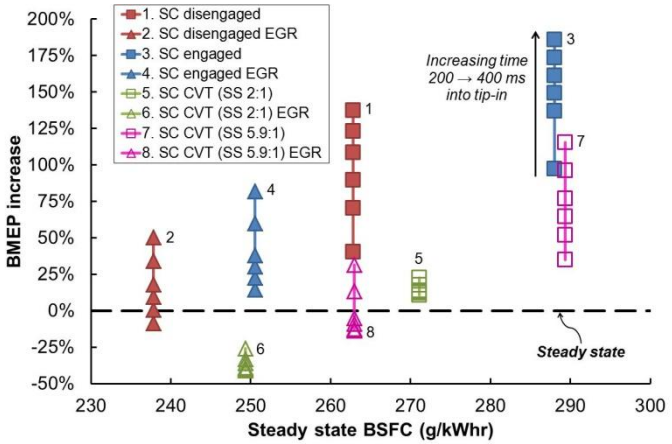

Figure 19 – Driveability analysis – percentage BMEP increase at key times during tip-in transient against initial steady state BSFC